Oxygen Reduction Reaction

DOI: 10.1002/ange.201410258

Sulfur-Doped Graphene Derived from Cycled Lithium–Sulfur Batteries as a Metal-Free Electrocatalyst for the Oxygen Reduction Reaction**

Zhaoling Ma, Shuo Dou, Anli Shen, Li Tao, Liming Dai, and Shuangyin Wang**

Abstract: *Heteroatom-doped carbon materials have been extensively investigated as metal-free electrocatalysts to replace commercial Pt/C catalysts in oxygen reduction reactions in fuel cells and Li–air batteries. However, the synthesis of such materials usually involves high temperature or complicated equipment. Graphene-based sulfur composites have been recently developed to prolong the cycling life of Li–S batteries, one of the most attractive energy-storage devices. Given the high cost of graphene, there is significant demand to recycle and reuse graphene from Li–S batteries. Herein, we report a green and cost-effective method to prepare sulfur-doped graphene, achieved by the continuous charge/discharge cycling of graphene–sulfur composites in Li–S batteries. This material was used as a metal-free electrocatalyst for the oxygen reduction reaction and shows better electrocatalytic activity than pristine graphene and better methanol tolerance durability than Pt/C.*

The exploration of highly efficient and durable low-cost electrocatalysts for the oxygen reduction reaction (ORR) in fuel cells or in metal–air batteries to replace precious metal electrocatalysts, such as platinum (and its alloy), has triggered extensive research interest.[1] Electrocatalysts for ORR are key for the development of renewable energy technologies. Although Pt and its alloy remain the most efficient catalysts, its scarcity in nature leads to a high cost in practical applications. Additionally, the Pt catalyst often suffers from decreasing activity and a low tolerance to methanol which hinder the further development of fuel-cell technologies. Until now, alternatives based on non-precious metals or metal-free materials, such as heteroatom-doped/surface-modified carbon,[2] have been intensively investigated. Among all the metal-free electrocatalysts, heteroatom-doped carbon materials (e.g. carbon nanotubes, graphene, mesoporous carbon) are promising candidates for replacing Pt for the ORR in fuel cells.[3]

Recent progress has demonstrated that heteroatom doping of carbon-based materials showed promising metal-free electrocatalytic activities as a result of the charge polarization, which stems from the difference in electronegativity between carbon atoms and heteroatoms.[4] For example, we successfully prepared vertically aligned nitrogen-doped carbon nanotubes, showing higher electrocatalytic activity and better long-term stability compared to the commercial Pt/C electrocatalysts.[1c] Subsequently we developed graphene co-doped with boron and nitrogen (BCN graphene) and graphene co-doped with nitrogen and sulfur (NSG) to be used as ORR electrocatalysts.[5] Additionally, we have also developed the molecular-doping strategy using nitrobenzene with a strong electron-withdrawing ability to dope graphene as an efficient metal-free electrocatalyst for ORR.[2a] According to quantum-mechanical calculations, the origin of the improved activity for ORR using heteroatom-doped graphene could be attributed to the charge polarization induced by the heteroatom doping.[1c] More interestingly, although sulfur has a similar electronegativity value to carbon, sulfur-doped graphene also demonstrated enhanced electrocatalytic activity compared to pristine undoped graphene.[6] Baek et al. attributed the enhanced ORR activity of S-doped graphene to the "electron spin density" and concluded that the doped sulfur atoms and sulfur oxides (O=S=O) could strongly promote ORR activity.[4c] Although doped graphene or other carbon materials (including sulfur-doped graphene) showed enhanced ORR activity, the methods used to prepare doped graphene often involve tedious chemical vapor deposition (CVD), plasma treatment, or high-temperature annealing methods.[7] These methods usually involve high energy consumption and require harsh experimental conditions. Therefore, the development of a simple and eco-friendly method for the production of heteroatom-doped carbon-based materials with enhanced ORR electrocatalytic activity is highly desired.

Herein, we obtained S-doped graphene from a cycled lithium–sulfur battery in which graphene–sulfur composites were used as cathode materials (Scheme 1). The Li–S battery has garnered significant attention in recent years because of the large theoretical capacity of sulfur and the low environmental impact of the battery, aided by the high availability of resource materials for the cathode.[8] Despite these considerable advantages, there are still a number of challenges to be addressed in the optimization of Li–S batteries. First,

[*] Z. Ma, S. Dou, A. Shen, L. Tao, Prof. S. Wang
State Key Laboratory of Chem/Bio-Sensing and Chemometrics
College of Chemistry and Chemical Engineering
Hunan University, Changsha, 410082 (P.R. China)
E-mail: shuangyinwang@hnu.edu.cn
Prof. L. Dai
Department of Macromolecular Science and Engineering
Case Western Reserve University
10900 Euclid Avenue, Cleveland, OH 44106 (USA)
E-mail: liming.dai@case.edu

[**] We acknowledge the support from the National Natural of Science Foundation of China (Grant No.: 51402100), AFOSR MURI (FA9550-12-1-0037), National Science Foundation (IIP-1343270 and CMMI-133123), Youth 1000 Talent Program of China, and Inter-discipline Research Programme of Hunan University.

Supporting information for this article is available on the WWW under http://dx.doi.org/10.1002/anie.201410258.

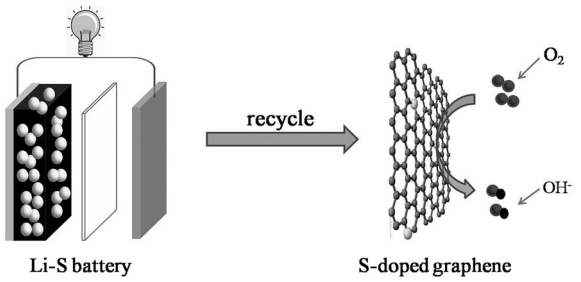

Scheme 1. Representation of the electrochemical doping of graphene by sulfur in Li–S batteries and its use in the oxygen reduction reaction. Sulfur atoms are represented by light-gray spheres in the battery and as dopant within the graphene.

elemental sulfur has a high electrical resistivity. Second, the polysulfide ions that are formed during the discharge/charge processes are highly soluble in organic solvent electrolytes. The soluble intermediate Li polysulfides can diffuse through the electrolyte to the Li anode where they are reduced to the final discharge products (solid precipitates Li_2S or Li_2S_2).[9] These issues can lead to a low utilization of active materials, a low columbic efficiency, and a short cycle life of the Li–S batteries. The most serious problem for Li–S batteries is its short cycle life. To address these challenges, various carbon materials such as graphene have been used to accommodate insulated sulfur so that its insulation properties may be overcome and the dissolution of Li polysulfides may be decreased, as reported by Nazar et al.[10] Although S–graphene composites have been developed to improve the cycle life of Li–S batteries, the current development is still far from commercialization.[11] Another critical issue is the high cost of graphene used in Li–S batteries based on graphene–sulfur composites. It will be very interesting to discover the potential applications of cycled graphene-based Li–S batteries. Herein, we successfully recycled graphene from a cycled Li–S battery and found that sulfur doping into graphene was achieved by the continuous charge/discharge cycling of the Li–S battery. The S-doped graphene, derived by this green and cost-efficient method, was used as a metal-free electrocatalyst for the oxygen reduction reaction, showing enhanced electrocatalytic activity.

In a typical sulfur–graphene-based Li–S battery, the sulfur–graphene composite (denoted as S–G) was prepared by the classical vapor infiltration method with sulfur powder and thermally exfoliated graphite oxide.[12] The mass percentage of sulfur in the S–G composite is determined to be 79.5 wt% (see Experimental Section in the Supporting Information). The three-dimensional structure of graphene was maintained after the sulfur loading/infiltration, as shown by the scanning electron microscopy (SEM) image in Figure S1 a and b in the Supporting Information. Additionally, Figure S1 b shows that no obvious bulk sulfur particles are formed. Transmission electron microscopy (TEM) images shown in Figure S2 confirm the uniform distribution of sulfur on the graphene surface. The as-prepared S–G composite was used as the cathode within the Li–S batteries. The electrochemical performance of the Li–S battery is shown in Figure 1. Typical cyclic voltammetry curves collected within

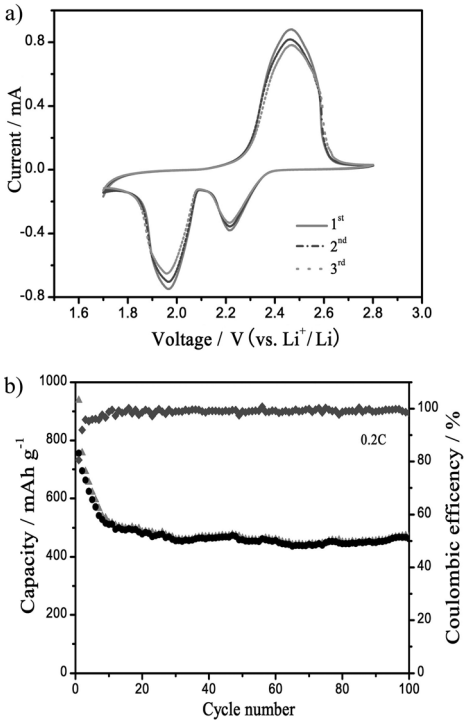

Figure 1. a) Cyclic voltammogram of the cathode (composed of a sulfur–graphene composite) in a Li–S battery at a scan rate of 0.1 mV s^{-1}. b) Cycle durability of S–G-based Li–S battery at a current rate of 0.2 C.

a voltage window from 1.7 to 2.8 V at a scan rate of 0.1 mV s^{-1} are given in Figure 1 a. The two cathodic peaks detected at 2.22 and 1.96 V correspond to a two-stage reduction process. The first stage is the transition from elemental sulfur to lithium polysulfides (Li_2S_n, $4 < n < 8$) and the second stage can be attributed to the further reduction of these polysulfides to form Li_2S_2/Li_2S. The cycling performance of the S–G composite at a current density of 0.2 C (1C = 1675 mAh g^{-1}) is shown in Figure 1 b, which is similar to that measured for typical Li–S batteries based on sulfur–graphene composites.

The S–G-based Li-S batteries were cycled for 100 cycles. The batteries were subsequently disassembled in order to recycle the graphene materials by removing elemental sulfur, polysulfides, and binder (the as-recycled graphene was denoted as SG). Thermally exfoliated graphene was employed to load sulfur under vacuum conditions and the sulfur–graphene composite was obtained with a homogeneous distribution of sulfur, as shown in Figure S2. After 100 cycles, the recycled graphene has a clean surface, as shown by the TEM image of SG in Figure S3, confirming that the elemental sulfur and other impurities were removed by the thorough rinsing. X-ray photoelectron spectroscopy (XPS) analysis was performed to identify the composition and the chemical state of the recycled S–G material. Figure S4 a shows the high-resolution C 1s spectrum for the recycled SG from Li–S batteries, which was deconvoluted into four peaks. It is clear that the carbon peak at 284.6 eV becomes more asymmetric and broadens as a result of S incorporation into the sp^2 network of graphene upon Li–S battery cycling. The

peak located at 285.8 eV corresponds to the C–O or C–S bond.[12,13] Additionally, the fine-scanned high-resolution S 2p spectrum shown in Figure S4b has a S $2p_{1/2}$ and S $2p_{3/2}$ doublet detected at 164.5 eV and 163.5 eV spin-orbit levels with an energy separation of 1.0 eV and an intensity ratio of about 1:2. These signals can be attributed to the formation of C=S and C–S bonds, respectively, further confirming the doping of the graphene network by sulfur. The peaks at 166–172 eV corresponding to -C-SO_X-C- possibly originate from the oxidic sulfur species. It should be pointed out that S^{2-} species were detected on the SG sample as shown in Figure S4b, probably because of the residual polysulfides. Cheng and coworkers[13] have demonstrated that the polysulfide-like S^{2-} species can induce charge transfer from S^{2-} to graphene. This charge-transfer behavior from S^{2-} to graphene might alter the electronic and oxygen-adsorption properties, which may cause an enhancement of the electrocatalytic activity for ORR as we reported previously.[1d]

Raman spectroscopy is a useful tool to investigate the electronic properties of carbon-based materials. The Raman spectra (Figure 2) show that the D band and the G band were

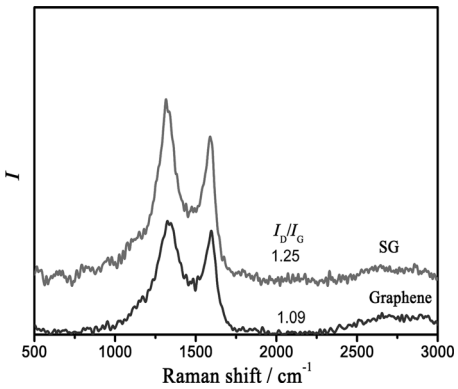

Figure 2. Raman spectra of graphene (black plot) and the as-recycled graphene SG (gray plot).

located around 1330 cm^{-1} and 1580 cm^{-1}, respectively. It has been found that the G band arises from the bond stretching of all sp^2-bonded pairs, including C–C and S–C, while the D band is associated with the sp^3-hybridized defect site.[14] In the Raman spectra of carbon-based materials, the parameter I_D/I_G is an interesting indicator of the level of defects within the material. From Figure 2, SG shows a higher I_D/I_G value than pristine graphene (1.25 for SG vs. 1.09 for graphene), confirming the atomic doping of sulfur into the graphene network.[15] Therefore, characterization both by XPS and Raman spectroscopy confirmed that by cycling Li–S batteries, graphene had been successfully doped with sulfur. Although the mechanism behind the doping is not clear, electrochemical doping has been previously proposed to dope graphene with heteroatoms.[16] Qu et al. prepared N-doped graphene through the electrochemical doping strategy in the presence of ammonia ions as the N source.[16] Sulfur-doped graphene has been previously prepared by the thermal annealing of graphene oxide in the presence of H_2S or CS_2, in which S^{2-} acted as the active site for the doping process.[17] Correspondingly, polysulfide species (S^{x-}) generated during the charge/discharge process of Li–S batteries might act as the active sites to promote sulfur doping. It is believed that the repeated charge/discharge process could promote doping of the graphene network with sulfur.

Previously, it has been demonstrated that sulfur-doped carbon materials could find potential application as metal-free electrocatalysts for the oxygen reduction reaction.[4c,6] To demonstrate the electrochemical performance of the as-recycled sulfur-doped graphene (SG), the electrocatalytic activity of SG was evaluated in the ORR in alkaline medium and was compared to undoped pristine graphene and the commercial Pt/C electrocatalysts. The cyclic voltammograms (CVs) for oxygen reduction on undoped graphene (Figure 3b) and doped SG electrodes (Figure 3a) at a constant active mass loading (0.01 mg) in an aqueous O_2-saturated KOH solution (0.1M). Both SG and graphene show a substantial reduction process in O_2-saturated 0.1M KOH solution, whereas no obvious response was detected in N_2-saturated solution. The onset potential of oxygen reduction for the pure graphene electrode is at −0.21 V versus SCE (saturated calomel electrode) with the cathodic reduction peak detected at approximately −0.40 V. Upon doping of the graphene with sulfur by cycling the Li–S batteries, both the onset potential and the ORR reduction peak potential shifted positively to around −0.15 V and −0.34 V, respectively. These results clearly demonstrated a significant enhancement in the ORR electrocatalytic activity for the doped SG with respect to the pure graphene electrode.[1e]

Linear-sweep voltammetry (LSV) measurements were performed to further investigate the ORR performance of SG and graphene on a rotating-disk electrode (RDE) in an O_2-saturated KOH solution (0.1M; Figure 3c). The half-wave potential derived from the LSV curve is a useful indicator to evaluate the catalytic activity of electrocatalysts. The half-wave potential of ORR at the undoped pristine graphene electrode is −0.43 V, whereas the ORR half-wave potential at the SG electrode shifted positively to −0.37 V with the limiting diffusion current higher than that of the graphene electrode. However, the electrocatalytic activity of the SG electrode toward ORR in terms of the onset potential and current density is still not as good as that of the commercial Pt/C electrocatalyst. RDE voltammetry measurements were undertaken to gain insight into the ORR performance of the graphene electrode before and after doping with sulfur. Figure S5 shows the LSV voltammograms at different rotation rates for the graphene and SG electrodes. Sulfur doping of graphene (SG) by cycling Li–S batteries led to better diffusion-controlled regions, as shown in Figure S5. The limiting current density increases with increasing rotation rate. The number of electrons transferred per O_2 molecule involved in the oxygen reduction reaction at both the graphene and SG electrodes was determined by the Koutecky–Levich (K–L) equation [Eq. (1)]:[1e]

$$\frac{1}{j} = \frac{1}{j_K} + \frac{1}{B\omega^{0.5}} \quad (1)$$

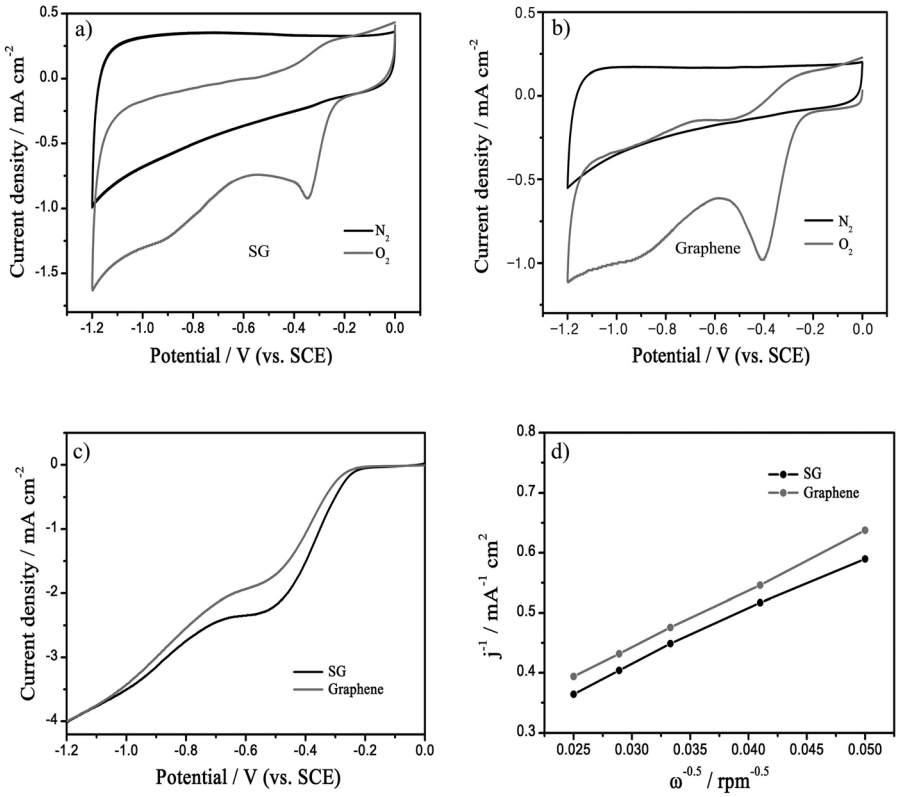

Figure 3. Cyclic voltammetry curves for oxygen reduction reactions on a) SG and b) graphene in N_2- and O_2-saturated KOH solution (0.1 M) at a scan rate of 50 mV s^{-1}. c) Linear sweep voltammetry curves of the ORR on SG and graphene in an O_2-saturated KOH solution (0.1 M) at 10 mV s^{-1} and a rotation rate of 1600 rpm. d) Koutecky–Levich plots for SG and graphene at −0.8 V.

where j_k is the kinetic current and ω is the rotating rate of the electrode. The parameter B could be determined from the slope of the K–L plots (Figure 3d) based on the Levich equation [Eq. (2)]:[9]

$$B = 0.2nF(D_{O_2})^{2/3}\nu^{-1/6}C_{O_2} \quad (2)$$

where n is the number of electrons transferred per oxygen molecule, F is the Faraday constant ($F = 96485$ C mol^{-1}), D_{O_2} is the diffusion coefficient of O_2 in 0.1M KOH ($D_{O_2} = 1.9 \times 10^{-5}$ cm^2 s^{-1}), ν is the kinetic viscosity (0.01 cm^2 s^{-1}), and C_{O_2} is the bulk concentration of O_2 ($C_{O_2} = 1.2 \times 10^{-6}$ mol cm^{-3}). The value 0.2 is employed when the rotation speed is expressed in rpm (revolutions per minute). K–L plots (Figure 3d) of SG and graphene can be calculated from the LSV voltammograms at −0.8 V in Figure S5. The plots of both SG and graphene show good linearity whereas SG shows a higher ORR current. These results further demonstrate that an electrode composed of SG with sulfur doping has a better ORR catalytic performance than an undoped graphene electrode. As calculated from the K–L plots, the number of electrons transferred (n) for SG is 3.13, higher than that calculated for graphene (2.90) at a potential of −0.8 V, indicating an efficient electron-transfer process for the oxygen reduction reaction on the SG electrode.

The possible crossover and stability of the SG electrode towards the ORR was tested by comparison with commercial Pt/C electrocatalysts. Cyclic voltammetry (CV) curves for the ORR on the SG electrode in the presence of methanol (0.1M) are compared with that of the commercial Pt/C electrocatalyst, as shown in Figure 4a and b. It is evident that the CV behavior of ORR on the SG electrode has not been affected, whereas the activity of the commercial Pt/C electrocatalyst suffered as a result of the typical methanol oxidation behavior. This result demonstrates that the SG electrocatalyst has excellent fuel selectivity for ORR activity compared to the commercial Pt/C electrocatalyst. The durability of the SG electrocatalyst is measured by comparison with the commercial Pt/C electrocatalyst in an O_2-saturated KOH solution (0.1M), as shown in Figure 4c. The linear sweep voltammogram (LSV) of ORR on SG and graphene at 1600 rpm are collected before and after 2000 cycles of cyclic voltammetry cycled within the potential range of −0.8–0 V and at a scan rate of 100 mV s^{-1} (Figure 4c). The onset potentials of ORR on the SG electrocatalyst remains the same, whereas the onset potential of ORR on the commercial Pt/C electrocatalyst undergoes a noticeable shift in the negative (cathodic) direction after 2000 continuous cycles. This result further demonstrates that the SG electrocatalyst exhibits more stable electrocatalytic activity than the commercial Pt/C electrocatalyst.

In summary, using a green and cost-efficient strategy, we have successfully recycled S-doped graphene from cycled Li–S batteries and employed it as a metal-free electrocatalyst for the oxygen reduction reaction. The sulfur doping of graphene was realized by the continuous cycling of graphene–sulfur composites in the Li–S batteries, as confirmed by Raman and XPS analysis. The doping mechanism is believed to be similar to other electrochemical doping methods and requires further investigation to fully understand it. The SG electrocatalyst exhibits better electrocatalytic activity than pristine undoped graphene with a better fuel selectivity and more stable durability for oxygen reduction reactions. This recycled SG electrocatalyst could provide an efficient method to reuse graphene-based electrodes in Li–S batteries. These findings indicate that recycling S-doped graphene from graphene-based Li–S batteries could serve as a general approach to the cost-effective development of various carbon-based metal-free efficient ORR catalysts.

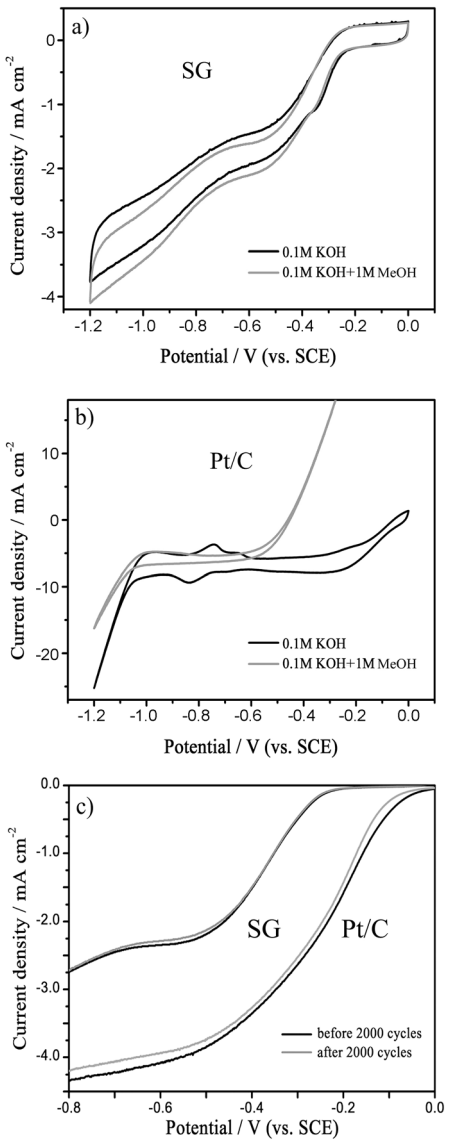

Figure 4. Cyclic voltammetry curves on a) the SG and b) Pt/C electrocatalysts at a scan rate of 100 mV s^{-1} in O_2-saturated KOH solution (0.1 M) and in O_2-saturated KOH solution (0.1 M) in the presence of methanol (1.0 M). c) Linear sweep voltammograms of ORR at 1600 rpm on SG and Pt/C before and after 2000 cycles of cyclic voltammetry running in O_2-saturated KOH solution (0.1 M) at a scan rate of 100 mV s^{-1}.

Received: October 20, 2014
Published online: December 5, 2014

Keywords: electrocatalysis · fuel cells · graphene · oxygen reduction reaction · sulfur doping

[1] a) L. Xiao, L. Zhuang, Y. Liu, J. T. Lu, H. D. Abruna, *J. Am. Chem. Soc.* **2009**, *131*, 602–608; b) V. R. Stamenkovic, B. Fowler, B. S. Mun, G. J. Wang, P. N. Ross, C. A. Lucas, N. M. Markovic, *Science* **2007**, *315*, 493–497; c) K. Gong, F. Du, Z. Xia, M. Durstock, L. Dai, *Science* **2009**, *323*, 760–764; d) S. Wang, D. Yu, L. Dai, *J. Am. Chem. Soc.* **2011**, *133*, 5182–5185; e) S. Wang, D. Yu, L. Dai, D. W. Chang, J.-B. Baek, *ACS Nano* **2011**, *5*, 6202–6209; f) S. Wang, E. Iyyamperumal, A. Roy, Y. Xue, D. Yu, L. Dai, *Angew. Chem. Int. Ed.* **2011**, *50*, 11756–11760; *Angew. Chem.* **2011**, *123*, 11960–11964.

[2] a) S. Dou, A. Shen, L. Tao, S. Wang, *Chem. Commun.* **2014**, *50*, 10672–10675; b) A. Shen, Y. Zou, Q. Wang, R. A. W. Dryfe, X. Huang, S. Dou, L. Dai, S. Wang, *Angew. Chem. Int. Ed.* **2014**, *53*, 10804–10808; *Angew. Chem.* **2014**, *126*, 10980–10984; c) X. Wang, J. Wang, D. Wang, S. Dou, Z. Ma, J. Wu, L. Tao, A. Shen, C. Ouyang, Q. Liu, S. Wang, *Chem. Commun.* **2014**, *50*, 4839–4842; d) Y. Li, W. Zhou, H. Wang, L. Xie, Y. Liang, F. Wei, J.-C. Idrobo, S. J. Pennycook, H. Dai, *Nat. Nanotechnol.* **2012**, *7*, 394–400.

[3] a) G. Tuci, C. Zafferoni, P. D'Ambrosio, S. Caporali, M. Ceppatelli, A. Rossin, T. Tsoufis, M. Innocenti, G. Giambastiani, *ACS Catal.* **2013**, *3*, 2108–2111; b) L. Qu, Y. Liu, J.-B. Baek, L. Dai, *ACS Nano* **2010**, *4*, 1321–1326; c) J. Xu, Y. Zhao, C. Shen, L. Guan, *ACS Appl. Mater. Interfaces* **2013**, *5*, 12594–12601.

[4] a) L.-F. Chen, X.-D. Zhang, H.-W. Liang, M. Kong, Q.-F. Guan, P. Chen, Z.-Y. Wu, S.-H. Yu, *ACS Nano* **2012**, *6*, 7092–7102; b) Z.-S. Wu, A. Winter, L. Chen, Y. Sun, A. Turchanin, X. Feng, K. Müllen, *Adv. Mater.* **2012**, *24*, 5130–5135; c) I. Y. Jeon, S. Zhang, L. P. Zhang, H. J. Choi, J. M. Seo, Z. H. Xia, L. M. Dai, J. B. Baek, *Adv. Mater.* **2013**, *25*, 6138–6145; d) I. Y. Jeon, H. J. Choi, M. Choi, J. M. Seo, S. M. Jung, M. J. Kim, S. Zhang, L. P. Zhang, Z. H. Xia, L. M. Dai, N. Park, J. B. Baek, *Sci. Rep.* **2013**, *3*, 1810–1817; e) I. Y. Jeon, H. J. Choi, S. M. Jung, J. M. Seo, M. J. Kim, L. M. Dai, J. B. Baek, *J. Am. Chem. Soc.* **2013**, *135*, 1386–1393.

[5] a) S. Wang, L. Zhang, Z. Xia, A. Roy, D. W. Chang, J. B. Baek, L. Dai, *Angew. Chem. Int. Ed.* **2012**, *51*, 4209–4212; *Angew. Chem.* **2012**, *124*, 4285–4288; b) See Ref. [2c].

[6] Z. Yang, Z. Yao, G. F. Li, G. Y. Fang, H. G. Nie, Z. Liu, X. M. Zhou, X. Chen, S. M. Huang, *ACS Nano* **2012**, *6*, 205–211.

[7] a) J. J. Zeng, Y. J. Lin, *Appl. Phys. Lett.* **2014**, *104*, 133506; b) See Ref. [3b].

[8] a) G. M. Zhou, S. F. Pei, L. Li, D. W. Wang, S. G. Wang, K. Huang, L. C. Yin, F. Li, H. M. Cheng, *Adv. Mater.* **2014**, *26*, 625–631; b) Y. C. Qiu, W. F. Li, W. Zhao, G. Z. Li, Y. Hou, M. N. Liu, L. S. Zhou, F. M. Ye, H. F. Li, Z. H. Wei, S. H. Yang, W. H. Duan, Y. F. Ye, J. H. Guo, Y. G. Zhang, *Nano Lett.* **2014**, *14*, 4821–4827; c) X. Yang, L. Zhang, F. Zhang, Y. Huang, Y. S. Chen, *ACS Nano* **2014**, *8*, 5208–5215; d) M. Q. Zhao, Q. Zhang, J. Q. Huang, G. L. Tian, J. Q. Nie, H. J. Peng, F. Wei, *Nat. Commun.* **2014**, *5*, 3410–3414.

[9] Q. Zhang, X. B. Cheng, J. Q. Huang, H. J. Peng, F. Wei, *New Carbon Mater.* **2014**, *29*, 241–264.

[10] a) X. L. Ji, K. T. Lee, L. F. Nazar, *Nat. Mater.* **2009**, *8*, 500–506; b) L. F. Nazar, M. Cuisinier, Q. Pang, *MRS Bull.* **2014**, *39*, 436–442; c) J. Schuster, G. He, B. Mandlmeier, T. Yim, K. T. Lee, T. Bein, L. F. Nazar, *Angew. Chem. Int. Ed.* **2012**, *51*, 3591–3595; *Angew. Chem.* **2012**, *124*, 3651–3655.

[11] S. Evers, L. F. Nazar, *Acc. Chem. Res.* **2013**, *46*, 1135–1143.

[12] C. X. Zu, A. Manthiram, *Adv. Energy Mater.* **2013**, *3*, 1008–1012.

[13] G. M. Zhou, L. C. Yin, D. W. Wang, L. Li, S. F. Pei, I. R. Gentle, F. Li, H. M. Cheng, *ACS Nano* **2013**, *7*, 5367–5375.

[14] See Ref. [2c].

[15] a) M. Bruna, A. K. Ott, M. Ijas, D. Yoon, U. Sassi, A. C. Ferrari, *ACS Nano* **2014**, *8*, 7432–7441; b) M. Kalbac, A. Reina-Cecco, H. Farhat, J. Kong, L. Kavan, M. S. Dresselhaus, *ACS Nano* **2010**, *4*, 6055–6063.

[16] Y. Li, Y. Zhao, H. H. Cheng, Y. Hu, G. Q. Shi, L. M. Dai, L. T. Qu, *J. Am. Chem. Soc.* **2012**, *134*, 15–18.

[17] H. L. Poh, P. Simek, Z. Sofer, M. Pumera, *ACS Nano* **2013**, *7*, 5262–5272.